E. Battaloğlu et al. / Hacettepe J. Biol. & Chem., 2023, 51 (4), 327-340

Research Article

Hacettepe Journal of Biology and Chemistry

journal homepage: www.hjbc.hacettepe.edu.tr

Comparison of the Glio-Protective Effects of Biopolymer Coated Electrospun Scaffolds

Biyopolimer Kaplı Elektroeğirilmiş Doku İskelelerinin Glio-Koruyucu Etkisinin Karşılaştırılması

Ece Battaloğlu[1], Zehra Gul Morçimen[2*], and Aylin Sendemir[1,2,3]

[1]Department of Bioengineering, Faculty of Engineering, Ege University, Bornova, Izmir, Turkey.

[2]Department of Bioengineering, Graduate School of Natural and Applied Sciences, Ege University, Bornova, Izmir, Turkey.

[3]Department of Biomedical Technologies, Graduate School of Natural and Applied Sciences, Ege University, Bornova, Izmir, Turkey.

ABSTRACT

Gliosis is a condition that plays a negative role in various neurological pathologies. In this study, it was aimed to obtain and compare the glio-protective effects of electrospun fibrous scaffolds coated by different biopolymers. First, the gliosis model was optimized by treatment with lipopolysaccharide (LPS) and interferon-gamma (IFN-γ) to induce a reactive change in human glioblastoma cells (U-87 MG) cells. The selected inducer was applied to U-87 MG cells grown on polycaprolactone (PCL), hyaluronic acid (HA)-coated, gelatin-coated, and collagen-coated PCL scaffolds. Immunofluorescent (IF) staining was performed by glial fibrillary acidic protein (GFAP) antibody to determine the level of gliosis. It was found that 5µg/mL LPS concentration induced gliosis and HA-coated PCL scaffolds have shown a protective effect against it.

Key Words

Gliosis, neural tissue engineering, electrospinning, glio-protective.

ÖZ

Gliozis çeşitli nörolojik rahatsızlıklarda olumsuz rol oynayan bir patolojik durumdur. Bu çalışmada elektroeğirme ile üretilmiş doku iskeleleri üzerine farklı biyopolimer kaplamaların glio-koruyucu etkilerinin karşılaştırılması amaçlanmıştır. İlk olarak gliosis modeli, U-87 MG hücrelerini indüklemek için lipopolisakkarit (LPS) ve interferon-gama (IFN-γ) muamelesiyle optimize edilmiştir. Belirlenen indükleyici, polikaprolakton (PCL), hiyalüronik asit kaplı, jelatin kaplı ve kolajen kaplı PCL doku iskeleleri üzerinde kültive edilen U-87 MG hücrelerine uygulanmıştır. Gliozis seviyesini belirlemek için glial fibril asidik protein (GFAP) antikoru ile immünofloresan (IF) boyama yapılmıştır. En yüksek gliozisin 5µg/mL LPS ile indüklendiği olduğu ve HA kaplı PCL iskelelerin gliozise karşı koruyucu etkisi olduğu gösterilmiştir.

Anahtar Kelimeler

Gliozis, sinir doku mühendisliği, elektroeğirme, glio-koruyucu.

Article History: Feb 1, 2023; Revised: Jul 28, 2023; Accepted: June 8, 2023; Available Online: Oct 15, 2023.

DOI: https://doi.org/10.15671/hjbc.1245678

Correspondence to: A. Sendemir, Department of Bioengineering, Faculty of Engineering, Ege University, Bornova, Izmir, Turkey.

E-Mail: aylin.sendemir@ege.edu.tr

INTRODUCTION

Central and peripheral nerve damage and neurodegenerative diseases are critical and important health problems that significantly affect the quality of life. They burden health systems due to restricted and limited treatment options. Nerve damage causes severe psychological trauma while affecting motor functions that greatly limit normal daily activities, and recovery is a rare condition. It is not possible for patients to fully recover from CNS damage causing different neurodegenerative diseases such as Alzheimer's, Parkinson's, Huntington's Diseases, multiple sclerosis (MS), and epilepsy with currently available treatments [1,2]. For this reason, there is a need for new-generation studies in the field of neural tissue engineering [1,3–5].

The central nervous system (CNS) comprises the brain and the spinal cord, and the majority of neural tissue in the central nervous system comprises two cell types, neuronal cells, and glial cells. Among the glial cells are different support cells, including astrocytes, microglia, and oligodendrocytes. Gliosis is a condition that occurs in glial cells due to external or internal damage to the CNS. In pathological conditions, astrocytes become active, characterized by unnatural morphology with reactive astrogliosis [1]. In the damaged areas, normal tissue is replaced by connective tissue and forms a glial scar [1,3]. It is known that glial scar is observed in the tissue after spinal cord injury and the main pathology of glial scar is based on the gliosis mechanism [6]. Gliosis is an important obstacle in neuroregeneration, as well as the development of nerve tissue engineering technology. Various modifications are required to eliminate gliosis in the integration of scaffolds developed for nervous tissue [7]. Leach et al. have been able to largely circumvent this problem by a bioactive coating, attracting primary CNS neurons and promoting neurite outgrowth, while repelling primary astrocytes, meningeal cells, and fibroblasts. Many methods for the modification of scaffolds have been reported in the literature [8–11]. Yeh et al. reported that the collagen-based scaffolds they developed against glial scar formation decreased the expression of GFAP and anti-chondroitin sulfate and provided controlled astrocyte proliferation [12]. In a study with self-assembled peptides (SAPs), it was reported that inflammation and glial scarring were reduced, and functional recovery was facilitated with this tissue-engineered product [13].

Many methods are used to produce tissue scaffolds for tissue engineering, the most common of which is electrospinning, a fast, inexpensive, and efficient fiber scaffolding method. Electrospinning is a fiber production method obtained by drawing polymer solutions with an electric field from the tip of a needle to a grounded collector. Electrospun nanofiber scaffolds have much superiority, such as high surface area: volume ratio for cell interaction, steerable pore structure, high porosity, elastic surface properties, superior mechanical properties, and physical similarity to the natural extracellular matrix (ECM) structure. In order to successfully produce a functional tissue, the designed scaffolds must be able to mimic the ECM, provide oxygen and nutrient circulation to the tissue, and remove metabolic wastes during tissue regeneration [14–19]. PCL, a synthetic polymer, is highly advantageous in that it is biocompatible, biodegradable, highly elastic, has low toxicity, good mechanical properties, and has a slow degradation profile [20]. As a result of extensive in vitro and in vivo studies, PCL has been approved by the FDA for many medical and drug delivery devices [20].

A method applied to tissue engineering scaffolds to reduce glial scar and foreign body reactions is coating the scaffolds with bioactive compounds. HA, which has been shown to increase fibrin matrix formation and have a low risk of cytotoxicity, is a polymer that can be a candidate for these coatings. HA is a bioabsorbable glycosaminoglycan composed of linear polysaccharides and one of the main components of the extracellular matrix in all living organisms. Due to their unique viscoelastic properties and good biocompatibility, unmodified and derived HAs are widely used for drug delivery, encapsulation in cell domains, and tissue regeneration [21,22]. Özaydın et al., have shown the reduction of myelin degeneration along with the increase in the axon regeneration by HA coating on silicone tubes in *in vivo* rat models with experimental peri and epineural neuropathy [23].

Collagen, as an FDA approved polymer for clinical use in neural tissue engineering [24], is also used as a scaffold in combination with other polymers and proteins or as a modification agent [25]. Cao et al. developed a novel functional scaffold consisting of linearly ordered collagen scaffold (LOCS) fibers cross-linked by laminin and laminin-binding domain-ciliary neurotrophic factor (LBD-CNTF), and tested it in the rat transected sciatic nerve model. Results showed enhanced nerve regeneration as well as functional recovery [25].

Gelatin, another polymer that draws attention in neural tissue engineering studies, is a denatured protein obtained by the hydrolysis of animal collagen. The combination of gelatin/PCL promotes neurite outgrowth and Schwan cell (SC) proliferation *in vitro* [26,27] and *in vivo* [28]. Moreover, gelatin nanoparticles have been also used for neural tissue engineering [29]. Alvarez-Perez et.al has shown increased neural growth on nanoscale electrospun PCL membranes reinforced with gelatin in *in vitro* culture of PC-12 neural cells [27].

In this study, gliosis, which plays a devastating role in many neurological pathologies, was examined. One of the most commonly used cells for research on gliosis is U-87 MG human glioblastoma cells [30]. The greatest importance of this cell line is its success in reflecting human physiology. When induced, they begin to increase filament proteins on their surface, expand and show abnormal morphology. So this feature also meets our expectations from the cell to be used as a gliosis model [1,3]. GFAP is the main intermediate filament protein in astrocytes [31]. The upregulation of GFAP expression is known as a sensitive and reliable marker of reactive astrocytes [32]. LPS and IFN-γ were used separately to induce gliosis in U-87 MG cells [33]. LPS is the main component of the outer membrane of gram-negative bacteria such as Escherichia coli [34] and LPS-stimulated glia is a commonly used *in vitro* model to mimic neuroinflammatory states [33]. LPS has also been shown to induce U-87 MG cell chemotaxis [35]. IFN-γ is a key mediator in the pathological changes observed in many demyelinating diseases, including MS. It has been found that apoptosis is induced in U-87 MG cells treated with IFN-γ [36,37]. It was shown that IFN-γ is an important intermediary of gliosis observed in pathological conditions of the adult CNS [36].

This study aimed to determine the most ideal agent to induce gliosis in the U-87 MG cell line. The gliosis-inducing potential of LPS and IFN- γ was examined, and the concentration was optimized. Then, the PCL scaffold produced by electrospinning was coated with HA, gelatin, and collagen, which were thought to have the potential to prevent and/or reduce gliosis formation, and the glio-protective effects of the coatings were examined using GFAP antibody.

MATERIALS and METHODS

Culture of U-87 MG cells

U-87 MG cells were incubated in 5% CO_2 and 95–98% humidified atmosphere at 37°C. Dulbecco's Modified Eagle's Medium F-12 (DMEM/ F-12) (Capricorn, DMEM-12-A, CP22-5071, Germany) supplemented with 10% (v/v) fetal bovine serum (FBS, 0111:B410270-10b, 0111:B4, USA) and 0,1% (v/v) penicillin-streptomycin (1103E, Merck, Germany) was used as the culture medium. Cells were trypsinized by 0.25 % (v/v) trypsin–EDTA (2477340, Gibco, USA) every 2–3 days and passaged before reaching 85% confluency.

Development of gliosis in U-87 MG cell culture

Cells were cultured in 24-well culture dishes at a concentration of 10^5 cells/mL and were allowed to adhere to the surface for one night. Then, 6 experimental groups were formed by applying 100 ng/mL human IFN-γ (I17001, Sigma, USA) [36,37] and different LPS (0111:B4, Merck, USA) concentrations (0.5 µg/mL, 1 µg/mL, 2 µg/mL, 5 µg/mL, 10 µg/mL) [30,34] to the cells. At the end of 3 days, inducing factors were compared by performing IF staining.

Demonstration of gliosis by IF staining

Fixation was initiated by methanol (34860, Riedel-de Haën, US) for 30 minutes at -20 ºC. After washing 3 times for 5 minutes with Ca^{+2}, Mg^{+2}-free PBS containing 0.2% (v/v) Triton X-100 (Sigma, 9002-73-1, USA) and washing with 1% (w/v) BSA- Ca^{+2}, Mg^{+2}-free PBS (A9647, Sigma, USA) for 5 minutes, the primary antibody (1:100) (Ab7260, Anti-GFAP, Abcam) was applied. Cells were kept in a moist, dark chamber on a shaker at 4 ºC overnight. On the second day, after washing 5 times for 5 minutes with Ca^{+2}, Mg^{+2}-free PBS, secondary antibody (1:500) (Ab150075, Donkey Anti-Rabbit IgG H&L, Alexa Fluor® 647), and DAPI (1:1000) were applied in a 37 ºC CO_2-free incubator on a shaker for 2 hours. After washing, the samples were transferred to 70% (v/v) ethanol at room temperature for 1 minute. Enough Moviol (475904, Calbiochem, Germany) was added to cover the surface, and images were captured by a fluorescent microscope.

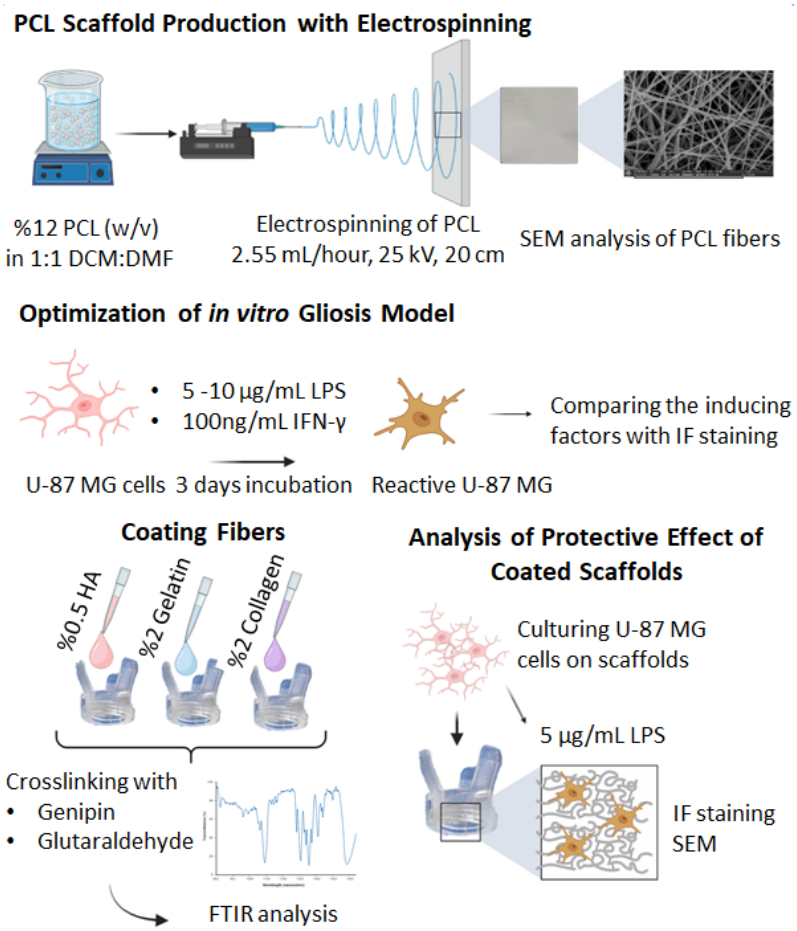

Figure 1. Graphical representation of the experimental procedure. Created with BioRender.comwavelength) is measured single layer (SL) and multi-layer coatings.

Obtaining fibrous scaffolds by electrospinning

12% (w/v) PCL (Sigma, 440744, USA) solution was prepared by dissolving in DMF (68-12-2, Sigma, USA) and DCM (75-09-2, Sigma, USA) at a 1:1 ratio. Electrospinning was performed with a 25 kV voltage difference and 20 cm collector-plate distance parameters at a flow rate of 2.55 mL/hr, as optimized according to previous works in our laboratory [38]. The obtained tissue scaffolds were cut to 1.5 cm x 1.5 cm and SEM images were taken at Ege University Central Research Test and Analysis Laboratory Application and Research Center (EGE-MATAL).

Coating the fibrous tissue scaffolds

Cut scaffolds were inserted into CellCrown inserts (C00006N Scaffdex 24NX). Crosslinking with genipin and glutaraldehyde was tested to stabilize water-soluble biopolymer coatings. A stock solution was prepared by dissolving 1 mg of genipin (Sigma, 6902778, Sigma, USA) in 1 mL of DMSO (67-68-5, BioShop, Canada). Solutions of 0.5% (w/v) HA (BGM280817-4, Bugamed, Turkey) and 2% (w/v) gelatin (1.04078.1000, Merck, Germany) were prepared in 0.5 mM genipin. 2% (w/v) collagen (9007-34-5, Sigma, USA) solution in 0.5 mM genipin containing 0.01M HCl (7647-01-0, Riedel-de Haën, US) has been prepared. The solutions were dripped onto the scaffolds and left to dry in an incubator overnight. In cross-linking with glutaraldehyde, 0.5% (w/v) HA and 2% (w/v) gelatin were dissolved in distilled water and 2% (w/v) collagen was dissolved in 0.01M HCl. The solutions were dripped onto the scaffolds and allowed to dry overnight in a CO_2-free incubator. The dried coated scaffolds were exposed to glutaraldehyde vapor overnight in a vacuum desiccator. After washing once with PBS for 5 minutes and twice with distilled water for 5 minutes, they were left to dry in the incubator overnight.

Characterization of coated tissue scaffolds with SEM and FTIR

SEM analysis and FTIR spectra were carried out at EGE-MATAL. SEM analyses were performed to determine the fiber properties of the scaffolds. Before SEM analy-

sis, the samples were coated with 80% gold and 20% palladium. SEM analyses of the scaffolds were carried out in Thermo Scientific Apreo S. Fiber diameter analysis was performed using open-source ImageJ software [39].

The samples were sent for FTIR spectra. Perkin Elmer Spectrum Two FTIR spectrometer was used to measure the spectra within the frequency range of 1850-550 cm^{-1}. Graphical interpretation was made and the most suitable cross-linking method was selected.

Application of the gliosis model on scaffolds

Coated scaffolds sterilized with ethylene oxide and placed into 24-well culture plates were conditioned in the culture medium overnight. U-87 MG cells were seeded at a concentration of 10^5 cells/scaffold and after 24 hours, LPS was applied for 3 days.

Cell Viability Analysis

The viability analysis was performed using Alamar Blue (30025-1, Biotium, USA). This analysis works with the principle that cells metabolize the resazurin chemical in the dye content and convert it into a chemical called resafurin, which is released out of the cell, and allows absorbance measurements at 570 nm and 600 nm [40]. The medium in the well was discarded and replaced by 90% culture medium, and 10% Alamar dye. After waiting for 4-5 hours, 100 µL was transferred to a 96-well culture dish, and the reading was made in the spectrophotometer. Fresh medium was put back into the culture dish to continue the culture period.

Comparison of glio-protective effects on different types of coatings by IF staining

IF staining was used both to confirm the gliosis in U-87 MG cell culture and to compare the protective effects of biopolymer coatings against gliosis.

Mean Fluorescence Intensity Analysis

The mean fluorescence intensity values on the IF-stained images were measured using ImageJ. Then, the DAPI stainings were photographed from the same region, and the fluorescence intensity was measured in the same way. The obtained GFAP fluorescent intensity values were normalized by the DAPI intensity levels.

Preparation of Scaffolds with Cells for SEM

Samples were washed by PBS for 30 sec. 1 M sodium cacodylate (C0250, Sigma, Germany) solution was prepared in distilled water. After fixing in 5% (v/v) glutaraldehyde, samples were kept in 1 M sodium cacodylate solution containing 7% (w/v) sucrose for 30 minutes. 2% (w/v) osmium tetroxide (19134, Electron Microscopy Sciences, UK) in 1 M sodium cacodylate was added and left for 30 minutes. After samples were washed with distilled water for 5 minutes they were dehydrated by alcohol series (35, 50, 70, 85, 95, 100, 100 %(v/v)) for 5 minutes each. Then the samples were kept in HMDS (999-97-3, Sigma, USA) solution for 15 minutes, and were left to dry. Before SEM analysis, the samples were coated with 80% gold and 20% palladium.

Statistical analysis

All quantitative experiments were carried out with at least three replications, and at least three samples from each experimental group were tested (n=3). The mean values and standard deviations were reported in the numerical evaluations. It was examined whether the results obtained from the experimental groups fit the normal distribution, and according to the results of this analysis, parametric (T-tests and ANOVA) statistical analysis methods were selected and applied at a 95% confidence interval. All statistical analyzes were performed and all graphs were created using the GraphPad program.

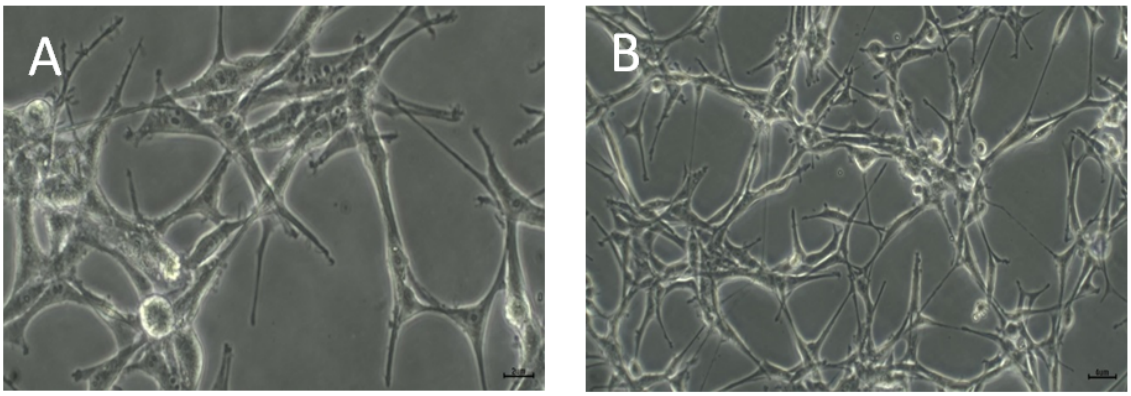

Figure 2. Morphological image of U-87 MG cells used in the study A) 20x magnification B) 10x magnification. U-87 MG cell morphology was consistent with the literature.

RESULTS and DISCUSSION

Morphology of U-87 MG Cell Line

Morphological observations of cells under appropriate culture conditions were made using inverted phase-contrast light microscopy (Figure 2). U-87 MG cell morphology was consistent with the literature [41].

Gliosis Model

IF staining was performed after 3 days of 0.5 µg/mL, 1 µg/mL, and 2 µg/mL, 5 µg/mL, 10 µg/mL LPS, and 100ng/mL IFN-γ treatment. While there was not any difference in 0.5 µg/mL, 1 µg/mL, and 2 µg/mL LPS concentrations, at 5 µg/mL, 10 µg/mL LPS, and 100ng/mL IFN-γ treatments there was a change in GFAP expression (Figure 3). After the mean fluorescence intensity of the IF images were analyzed by the ImageJ program, it was observed that the highest gliosis was induced by 5 µg/mL LPS (Figure 4).

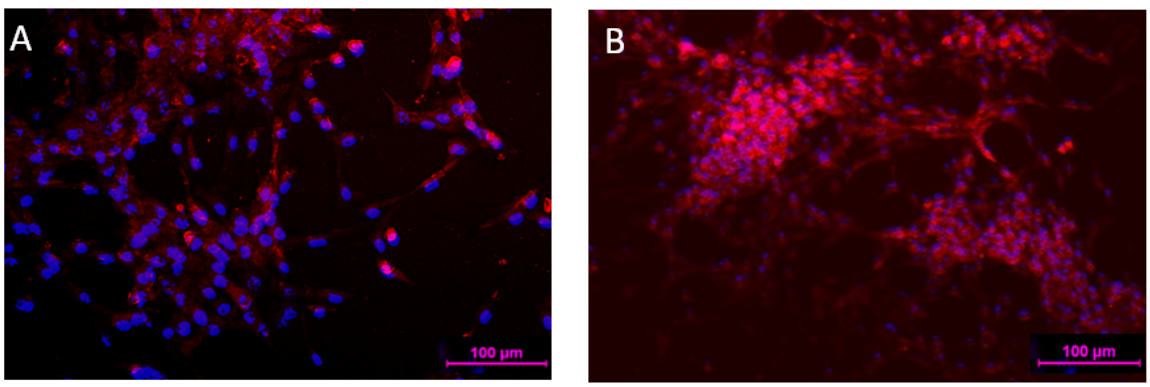

Figure 3. IF images A) Cell control, B) 5 µg/mL LPS induction, GFAP (red), DAPI (blue). Scale bar 100 µm. 5 µg/mL LPS caused higher IF staining compared to the control.

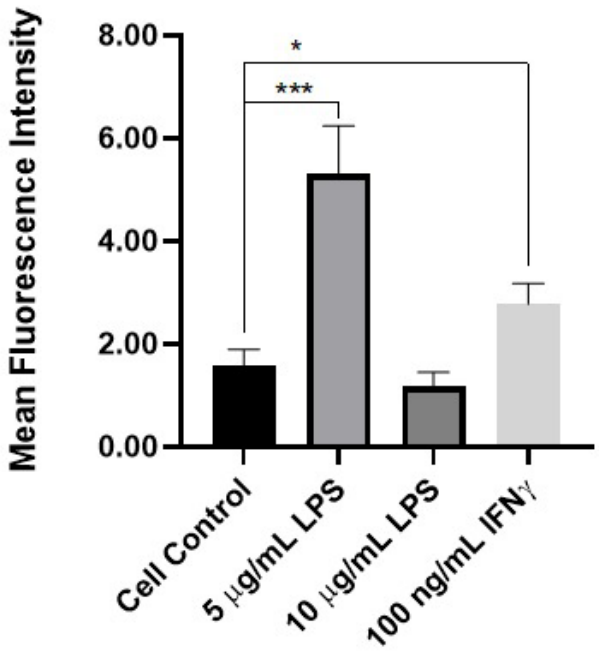

Figure 4. Normalized mean fluorescence intensity of IF images. A higher intensity level represents higher GFAP expression. The induction by 100 ng/mL IFN-γ and 5 µg/mL LPS was significantly higher than the control (* $p < 0.05$, *** $p < 0.005$). However, since 5 µg/mL LPS has the highest mean fluorescence intensity it was chosen as the gliosis-inducing agent.

Microstructural Analysis of Electrospun Scaffolds

The average fiber diameter obtained by SEM imaging was found to be 453.5 nm (Figure 5). At the same time, it is seen that there is no deterioration in the fiber structure of the obtained scaffolds and the fiber diameters were homogeneous.

Characterization of Scaffolds (FTIR)

Characteristic bands for HA for asymmetric stretch vibration of the carbonyl group of carboxylate ($COO–$) were found between 1500-1700cm^{-1} [42,43].

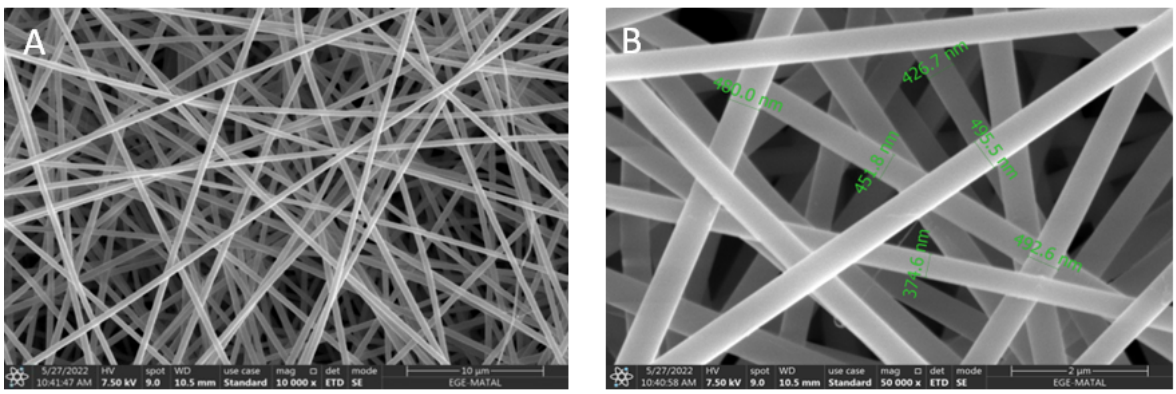

Figure 5. SEM images of PCL scaffolds. A) 10x magnification B) Fiber diameter measurements. The fibers were homogeneously distributed and no beadings were seen.

Characteristic bands of gelatin and collagen were exhibited at about 1650 cm^{-1}. These were associated with C=O stretching vibration and coupling of 1540 cm^{-1} N—H in planar bending [43,44].

Based on this information, typical bands were more pronounced on genipin cross-linking in PCL for both HA, gelatin, and collagen compared to glutaraldehyde (Figure 6). Therefore, the coating process on PCL scaffolds was carried out using genipin as the cross-linker.

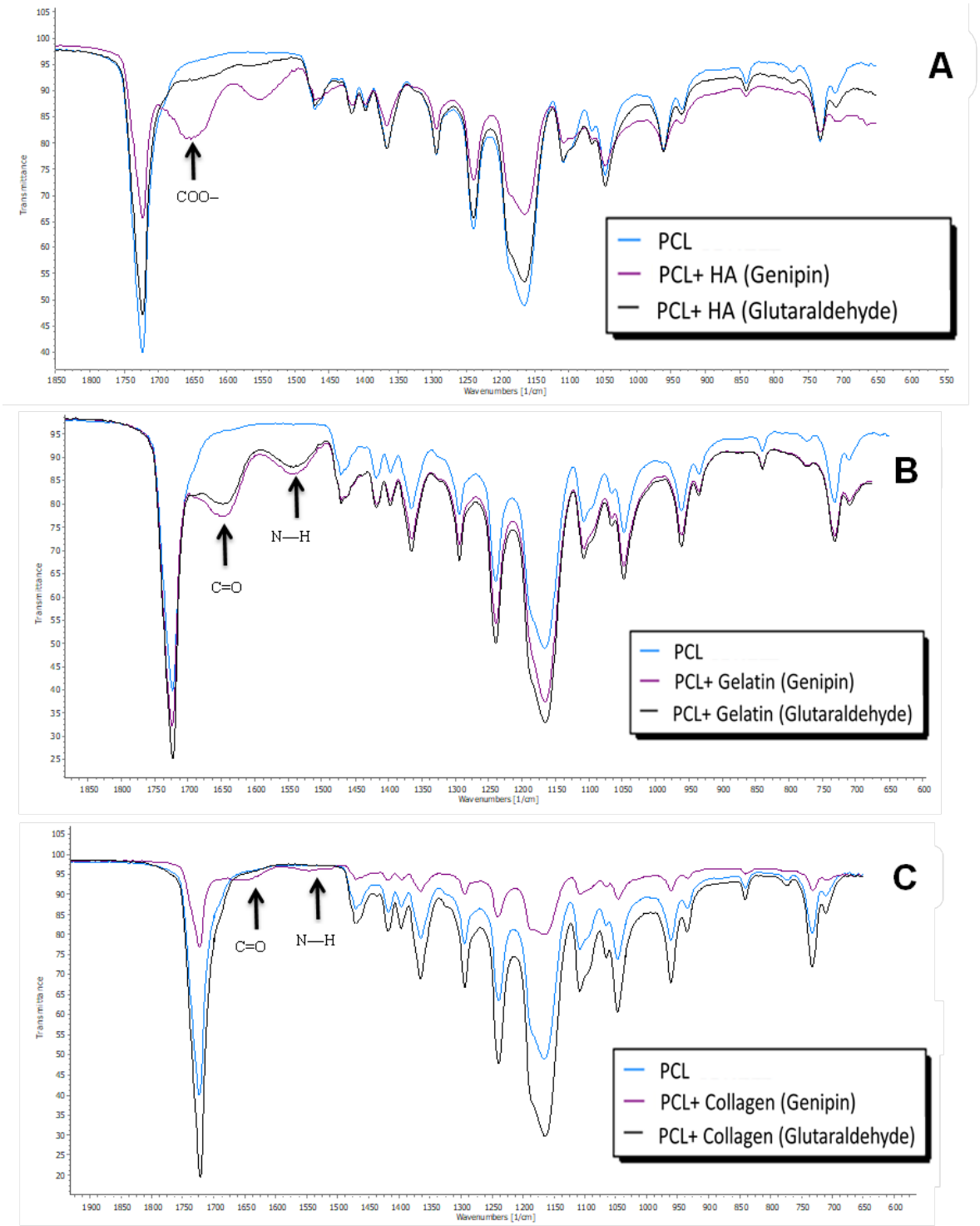

Figure 6. FTIR results of coated PCL scaffolds A) HA B) gelatin C) collagen.

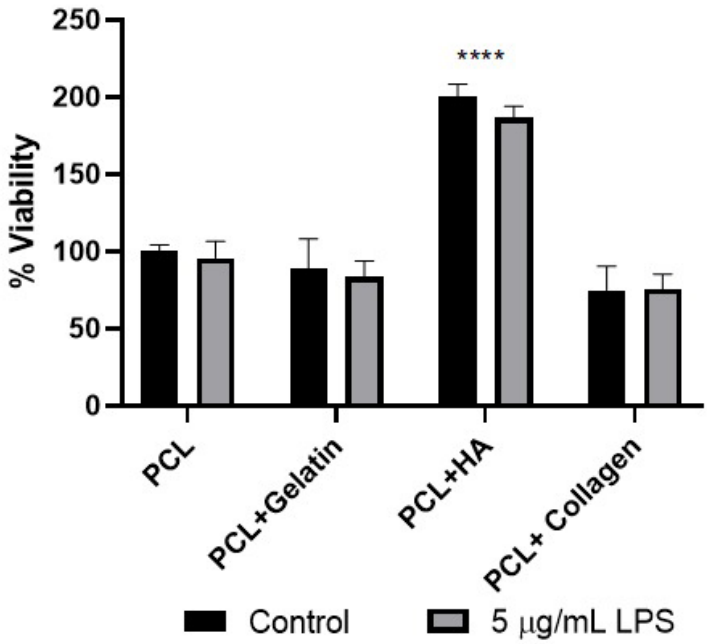

Figure 7. Cell viability results. There is a significant increase in cell viability on PCL+HA scaffolds compared to all other groups (**** $p < 0.001$).

Viability Analysis

It was seen that HA coating increased cell viability compared to the other scaffolds (Figure 7). In addition, 5 µg/mL LPS did not decrease cell viability.

Interpretation of Gliosis Recovery

PCL, HA-coated, gelatin-coated, and collagen-coated PCL scaffolds were compared. In SEM image analysis, it is seen that the cells were attached to the fibers.

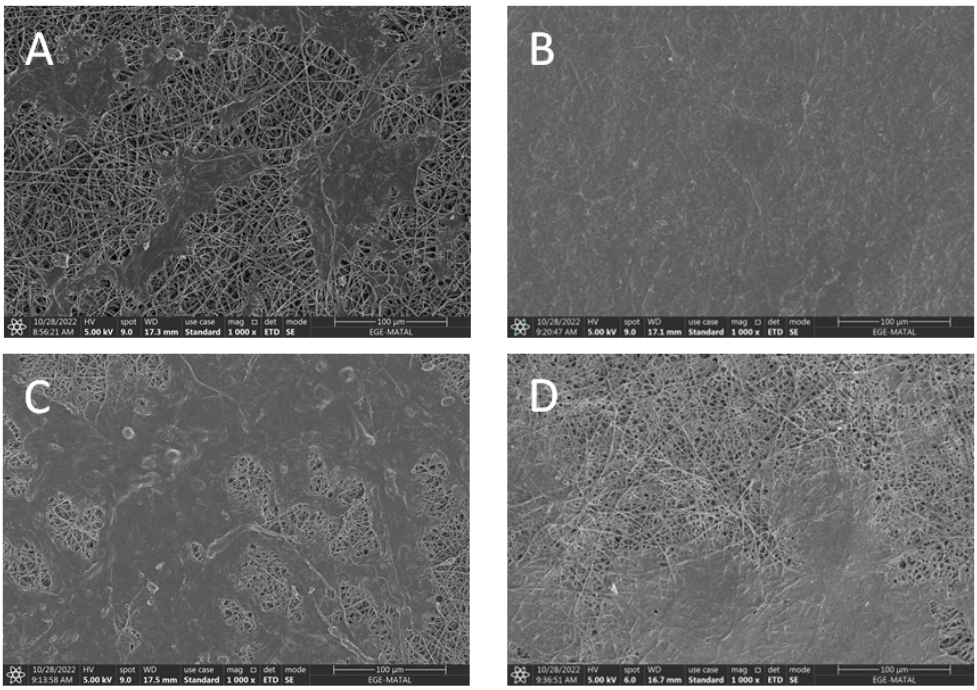

Figure 8. SEM images of U-87 MG cells on Scaffolds after 3 days. A) PCL, B) PCL+ HA, C) PCL+ gelatin, D) PCL+ collagen.

As a result of the IF staining performed to compare the glio-protective effects of the coatings, it was found that HA-coated PCL scaffolds showed the lowest normalized fluorescent intensity, and therefore the highest protective effect against gliosis (Figures 9 & 10).

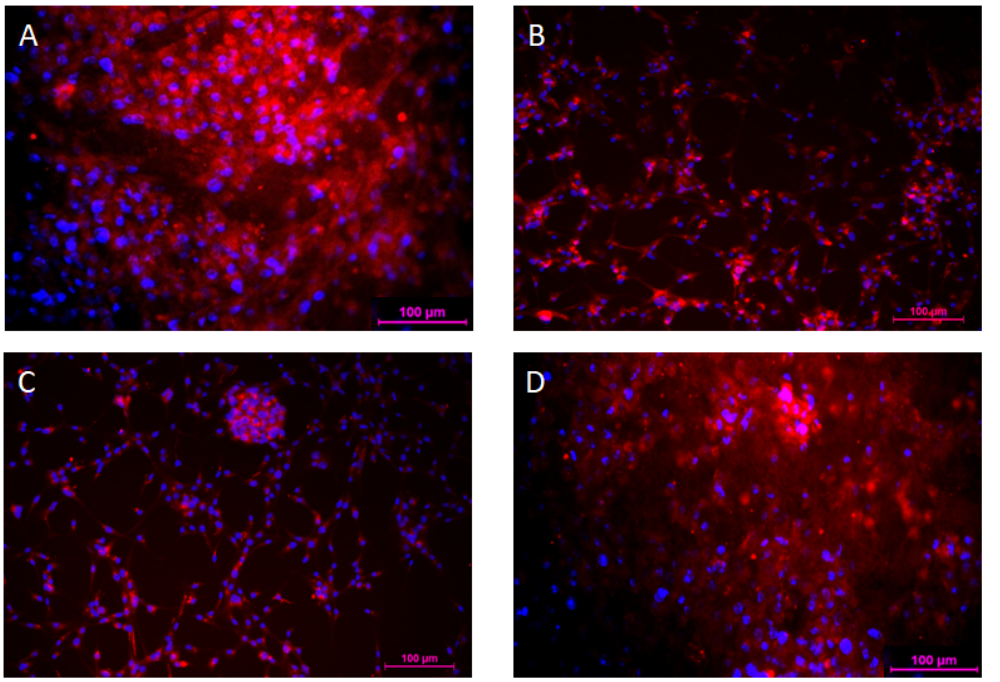

Figure 9. . IF images of scaffolds treated with 5 µg/mL LPS. GFAP (red), DAPI (blue). A) PCL, B) PCL+ HA C) PCL+ gelatin, D) PCL+ collagen Higher GFAP expression means higher gliosis. The lowest reactivity of astrocytes was observed on HA-coated PCL scaffolds.

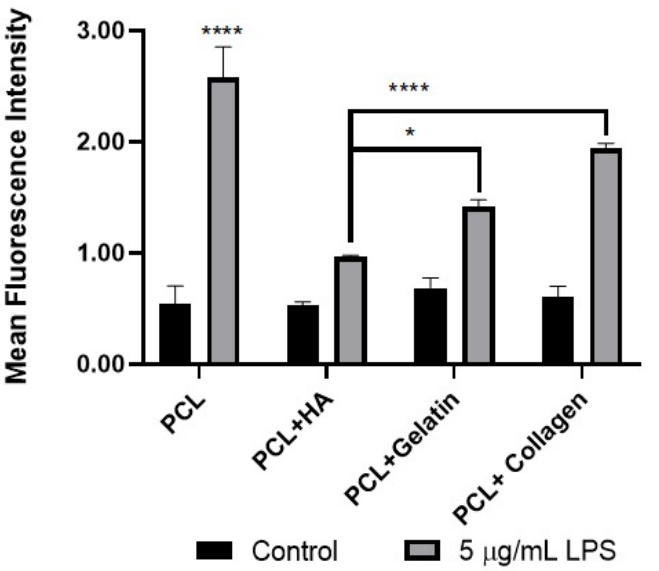

Figure 10. Normalized mean fluorescence intensity of GFAP IF images. A higher intensity level represents higher GFAP expression. HA-coated scaffolds showed lower GFAP expression and thus showed the highest glio-protective effect (* $p < 0.05$, **** $p < 0.001$).

DISCUSSION

The number of individuals with neurodegenerative diseases, which are very difficult to treat, is increasing day by day and this reduces the quality of life. In this study, gliosis, which plays a harmful role in neurological pathologies and is the basis of diseases such as stroke, drug abuse, Parkinson's, and Alzheimer's Disease, was investigated. For this purpose, it was aimed to create an *in vitro* model of gliosis on U-87 MG cells.

For induction of gliosis LPS trials were performed at 0.5 µg/mL, 1 µg/mL, and 2 µg/mL concentrations for 1 week, and during this period, the cells' morphological changes were regularly monitored daily. Although Huang et al. showed that treatment of U-87 MG with LPS (100 ng/mL) significantly increased expression of the astrocyte marker GFAP with simultaneous upregulation of SIGMAR1 expression [1], our results of IF staining were examined, no significant difference was observed at that concentration (no results given) on GFAP expression. LPS concentrations applied in *in vivo* studies is higher [45]. Although this study was *in vitro*, it was decided to increase the LPS concentration. Therefore, the experiment was repeated at 5 µg/mL and 10 µg/mL LPS concentrations. However, in line with the decrease in cell number at 10 µg/mL LPS, it was determined that apoptosis rather than gliosis was induced in cells. For this reason, 5 µg/mL LPS was chosen as the gliosis-inducing agent (Figure 3 and Figure 4). When the studies in the literature were examined, it was seen that IFN-γ was frequently preferred to create a gliosis model in recent years, and it was found that apoptosis was induced in U-87 MG cells treated with IFN-γ [46]. Based on this, induction was performed at a concentration of 100 ng/mL IFN-γ, and it was concluded that it also induced the gliosis model (Figure 4).

GFAP, which is the main intermediate filament protein in astrocytes and is known as a sensitive and reliable marker of reactive astrocytes, was used to characterize gliosis. All interpretations were made with the knowledge that a higher GFAP expression represents higher gliosis level [31,32]. Gliosis level was determined by processing the IF images with the ImageJ program. Looking at the data obtained (Figure 4), it was seen that induction by LPS at 5 µg/mL concentration and IFN-γ at 100ng/mL concentration was quite successful, and according to cell viability, the best result was obtained at 5 µg/mL LPS induction. Observation of the change in GFAP expression without decreasing the number of astrocyte cells indicates that gliosis was established at 5 µg/mL LPS induction (Figure 9 and Figure 10).

Along with the determination of the model, the glio-protective effects of PCL, HA-coated, gelatin-coated, and collagen-coated PCL scaffolds were also determined. It is very critical that the cells can adhere to the scaffold to be used. Therefore, tissue scaffolds were produced by the electrospinning method, which provides good cell adhesion and is frequently used in tissue engineering [14–19,47]. When looking at the SEM images of the PCL scaffold, the average value of the fiber diameters was 453.53 nm, and there was no deterioration in the fiber structures in the obtained scaffold and the fibers were homogeneous, which shows that electrospinning was successful as desired [14–16,18,19].

HA, gelatin, and collagen coatings were applied to the obtained fibrous PCL scaffolds in order to increase the attachment of cells, increase cell viability, and test the glio-protectivity. While preparing the coatings, glutaraldehyde, and genipin [48,49], which are frequently used in the literature, were preferred as cross-linkers and their comparisons were shown by FTIR spectra (Figure 6). It was seen that typical bands for HA have been found between 1500-1700cm^{-1} (carbonyl group of carboxylate (COO^{-})), for gelatin and collagen were exhibited at about 1650 cm^{-1}. These peaks were associated with C=O stretching vibration and coupling of 1540 cm^{-1} N—H in planar bending. The targeted peaks were clearer and higher when the genipin cross-linker was used, so the study was continued with genipin.

There is a significant increase in cell viability on PCL+HA scaffolds among all other groups (Figure 7). Collagen and gelatin did not have an effect on increasing the proliferation of U-87 MG. In addition, it is understood that LPS does not decrease cell viability at 5 µg/mL concentration. It shows that 5 µg/mL LPS only induced gliosis.

When looking at the IF images, the lowest average fluorescence intensity, therefore the lowest GFAP activity was observed on the HA-coated PCL scaffolds. This means that the most protective effect against gliosis was by the HA-coated PCL scaffolds.

HA is a polysaccharide that is found in the ECM prominently throughout the human body as a component of the ECM. Also, it is a primary component of the brain's

extracellular matrix and functions through cellular receptors to regulate cell behavior within the CNS [50]. HA is synthesized by neurons and astrocytes in the CNS and its localization and deposition occur around myelinated fibers and give rise to ECM substructures, called perineuronal nets [50,51]. It was shown that the decrease in HA concentration elicited a reduction in the total length of astrocytic processes and an increase in inflammatory markers in vitro [52]. The results support the hypothesis that HA inhibits glial scarring by decreasing gliosis [51]. HA plays a role in promoting cell motility and proliferation by integrating the receptors on the cell surface [51]. Proliferation may in part explain some of the spontaneous recoveries that occur in all CNS damages, which include spinal cord injury, excitotoxic injury, and ischemic [51].

The most notable gliosis model was obtained by 5µg/mL LPS concentration. Electrospun PCL scaffolds were successfully obtained at 25 kV voltage difference and 20 cm collector-plate distance at a flow rate of 2.55 mL/hour of 12% (w/v) PCL solution prepared by dissolving PCL in DMF and DCM at a 1:1 ratio. It was found that genipin was more effective as a cross-linker for coatings, and it was observed that the scaffolds that provided the highest glio-protective effect were HA coated PCL scaffolds. Thus, a contribution has been made to the literature on the importance of HA biopolymer in neuroscience, neural tissue engineering, and its protective effect on neurological pathologies such as gliosis.

Acknowledgments

We would like to thank BUGAMED BIOTECHNOLOGY for providing hyaluronic acid as a gift. Also, we would like to thank Prof. Dr. Ayse NALBANTSOY for her support in cell culture experiments. Zehra Gul MORCIMEN is supported by the TUBITAK-BIDEB 2211-A National Scholarship Program for Ph.D. Students and the YOK 100/2000 Scholarship in the field of smart and innovative materials.

References

1. R. Huang, Y. Zhang, B. Han, Y. Bai, R. Zhou, G. Gan, J. Chao, H. Yao, Circular RNA HIPK2 regulates astrocyte activation via cooperation of autophagy and ER stress by targeting MIR124-2HG, Autophagy, 13 (2017).
2. Y. Hu, H. Zhang, H. Wei, H. Cheng, J. Cai, X. Chen, L. Xia, H. Wang, R. Chai, Scaffolds with anisotropic structure for neural tissue engineering, Engineered Regeneration, 3 (2022) 154–162.
3. R.A.L. De Sousa, Reactive gliosis in Alzheimer's disease: a crucial role for cognitive impairment and memory loss, Metab Brain Dis, 37 (2022) 851–857.
4. M. Motavaf, • Majid Sadeghizadeh, • Mohammad Javan, Attempts to Overcome Remyelination Failure: Toward Opening New Therapeutic Avenues for Multiple Sclerosis, Cell Mol Neurobiol, 37 (n.d.).
5. S.C. Yetis, D.A. Ekinci, E. Cakir, E.M. Eksioglu, U.E. Ayten, A. Capar, B.U. Toreyin, B.E. Kerman, Myelin segmentation in fluorescence microscopy images, TIPTEKNO 2019 - Tip Teknolojileri Kongresi, (2019).
6. H. Wang, G. Song, H. Chuang, C. Chiu, A. Abdelmaksoud, Y. Ye, L. Zhao, Portrait of glial scar in neurological diseases, Int J Immunopathol Pharmacol, 31 (2018) 1–6.
7. Y. Wang, H. Tan, X. Hui, Biomaterial Scaffolds in Regenerative Therapy of the Central Nervous System, (2018).
8. Q. Zhang, B. Shi, J. Ding, L. Yan, J.P. Thawani, C. Fu, X. Chen, Polymer scaffolds facilitate spinal cord injury repair, Acta Biomater, 88 (2019) 57–77.
9. H. Yin, T. Jiang, X. Deng, M. Yu, H. Xing, X. Ren, A cellular spinal cord scaffold seeded with rat adipose-derived stem cells facilitates functional recovery via enhancing axon regeneration in spinal cord injured rats, Mol Med Rep, 17 (2018) 2998.
10. M. Li, H. Hu, Z. Yu, Y. Ding, Y. Wang, M. Wu, W. Qu, B. Chen, W. Shu, H. Tian, X. Ou, X. Zhang, Polymer-Based Scaffold Strategies for Spinal Cord Repair and Regeneration, (2020).
11. Z. Álvarez, A.N. Kolberg-Edelbrock, I.R. Sasselli, J.A. Ortega, R. Qiu, Z. Syrgiannis, P.A. Mirau, F. Chen, S.M. Chin, S. Weigand, E. Kiskinis, S.I. Stupp, Bioactive scaffolds with enhanced supramolecular motion promote recovery from spinal cord injury, Science (1979), 374 (2021) 848–856.
12. J.-Z. Yeh, D.-H. Wang, J.-H. Cherng, Y.-W. Wang, G.-Y. Fan, N.-H. Liou, J.-C. Liu, C.-H. Chou, A Collagen-Based Scaffold for Promoting Neural Plasticity in a Rat Model of Spinal Cord Injury, (n.d.).
13. Y. Liu, H. Ye, K. Satkunendrarajah, G.S. Yao, Y. Bayon, M.G. Fehlings, A self-assembling peptide reduces glial scarring, attenuates post-traumatic inflammation and promotes neurological recovery following spinal cord injury, (2013).
14. A. Jakobsson, M. Ottosson, M.C. Zalis, D. O'Carroll, U.E. Johansson, F. Johansson, Three-dimensional functional human neuronal networks in uncompressed low-density electrospun fiber scaffolds, Nanomedicine, 13 (2017) 1563–1573.
15. D. Doç Nimet Karagülle Mersin, Doku Mühendisliği Uygulamalari İçin Polivinil Alkol (Pva)/Nişasta Temelli Kriyojel Doku İskelelerinin Geliştirilmesi: Sentez, Karakterizasyon Ve Biyouyumluluk Değerlendirmeleri Doktora Tezi Seda Ceylan Mersin Üniversitesi Fen Bilimleri Enstitüsü Kimya Mühendisliği Anabilim Dali, N.D.
16. Y.L. Tezi, Marmara Üniversitesi Fen Bilimleri Enstitüsü Çok Girişli Elektroeğirme Yöntemiyle Nişasta/Pcl Kompozit Nanofiberlerin Üretilmesi Feyzanur (Bayrak) Sinar Metalurji Ve Malzeme Mühendisliği (Türkçe) Anabilim Dalı, N.D.

17. Bedir Tuba, Nöral Doku Mühendisliği İçin Doku İskelesi Tasarımı Ve Geliştirilmesi, n.d.
18. N. Zhang, U. Milbreta, J.S. Chin, C. Pinese, J. Lin, H. Shirahama, W. Jiang, H. Liu, R. Mi, A. Hoke, W. Wu, S.Y. Chew, Biomimicking Fiber Scaffold as an Effective In Vitro and In Vivo MicroRNA Screening Platform for Directing Tissue Regeneration, Advanced Science, 6 (2019).
19. N. Kaur, W. Han, Z. Li, M.P. Madrigal, S. Shim, S. Pochareddy, F.O. Gulden, M. Li, X. Xu, X. Xing, Y. Takeo, Z. Li, K. Lu, Y. Imamura Kawasawa, B. Ballester-Lurbe, J.A. Moreno-Bravo, A. Chédotal, J. Terrado, I. Pérez-Roger, A.J. Koleske, et al., Neural Stem Cells Direct Axon Guidance via Their Radial Fiber Scaffold, Neuron, 107 (2020) 1197-1211.e9.
20. M.O. Christen, F. Vercesi, Polycaprolactone: How a well-known and futuristic polymer has become an innovative collagen-stimulator in esthetics, Clin Cosmet Investig Dermatol, 13 (2020) 31–48.
21. F. Zamboni, M. Keays, S. Hayes, A.B. Albadarin, G.M. Walker, P.A. Kiely, M.N. Collins, Enhanced cell viability in hyaluronic acid coated poly(lactic-co-glycolic acid) porous scaffolds within microfluidic channels, Int J Pharm, 532 (2017) 595–602.
22. X. Lin, W. Wang, W. Zhang, Z. Zhang, G. Zhou, Y. Cao, W. Liu, Hyaluronic Acid Coating Enhances Biocompatibility of Nonwoven PGA Scaffold and Cartilage Formation, Https://Home.Liebertpub.Com/Tec, 23 (2017) 86–97.
23. I. Özaydin, E. Ünsaldi, Ö. Aksoy, S. Yayla, M. Kaya, M.B. Ulkay Tunali, A. Aktaş, E. Taşdemiroğlu, M. Cihan, B. Kurt, H.C. Yildirim, A. Şengöz, H. Erdoğan, Deneysel peri ve epinöral nörorafi uygulanmi{dotless}ş rat modellerinde silikon tüp ve silikon tüp + hyaluronik asit uygulamasi{dotless}ni{dotless}n adezyon formasyonuna etkisi, Kafkas Univ Vet Fak Derg, 20 (2014) 591–597.
24. X. Zhang, W. Qu, D. Li, K. Shi, R. Li, Y. Han, E. Jin, J. Ding, X. Chen, Functional Polymer-Based Nerve Guide Conduits to Promote Peripheral Nerve Regeneration, Adv Mater Interfaces, 7 (2020).
25. J. Cao, C. Sun, H. Zhao, Z. Xiao, B. Chen, J. Gao, T. Zheng, W. Wu, S. Wu, J. Wang, J. Dai, The use of laminin modified linear ordered collagen scaffolds loaded with laminin-binding ciliary neurotrophic factor for sciatic nerve regeneration in rats, Biomaterials, 32 (2011) 3939–3948.
26. G.K. Saraogi, P. Gupta, U.D. Gupta, N.K. Jain, G.P. Agrawal, Gelatin nanocarriers as potential vectors for effective management of tuberculosis, Int J Pharm, 385 (2010) 143–149.
27. M.A. Alvarez-Perez, V. Guarino, V. Cirillo, L. Ambrosio, Influence of gelatin cues in PCL electrospun membranes on nerve outgrowth, Biomacromolecules, 11 (2010) 2238–2246.
28. A. Kriebel, D. Hodde, T. Kuenzel, J. Engels, G. Brook, J. Mey, Cell-free artificial implants of electrospun fibres in a three-dimensional gelatin matrix support sciatic nerve regeneration in vivo, J Tissue Eng Regen Med, 11 (2017) 3289–3304.
29. M. Naseri-Nosar, S. Farzamfar, H. Sahrapeyma, S. Ghorbani, F. Bastami, A. Vaez, M. Salehi, Cerium oxide nanoparticle-containing poly (ε-caprolactone)/gelatin electrospun film as a potential wound dressing material: In vitro and in vivo evaluation, Materials Science and Engineering C, 81 (2017) 366–372.
30. F.K. Mediesse, T. Boudjeko, A. Hasitha, M. Gangadhar, W.F. Mbacham, P. Yogeeswari, Inhibition of lipopolysaccharide (LPS)-induced neuroinflammatory response by polysaccharide fractions of Khaya grandifoliola (CDC) stem bark, Cryptolepis sanguinolenta (Lindl) Schltr and Cymbopogon citratus Stapf leaves in raw 2647 macrophages and U87 glioblastoma cells, BMC Complement Altern Med, 18 (2018).
31. M. Potokar, M. Morita, G. Wiche, J. Jorgačevski, cells The Diversity of Intermediate Filaments in Astrocytes, (n.d.).
32. R. Helbok, R. Beer, Cerebrospinal fluid and brain extracellular fluid in severe brain trauma, Handb Clin Neurol, 146 (2018) 237–258.
33. D. Rampe, L. Wang, G.E. Ringheim, P2X7 receptor modulation of β-amyloid- and LPS-induced cytokine secretion from human macrophages and microglia, J Neuroimmunol, 147 (2004) 56–61.
34. T. Fath, D. Lecca, G. Pacheco-Lopez, A. Vargas-Caraveo, D.M. Hermann, M. Sardari, E. Dzyubenko, B. Schmermund, D. Yin, Y. Qi, C. Kleinschnitz, in collaboration with reviewer GP-L Dose-Dependent Microglial and Astrocytic Responses Associated With Post-ischemic Neuroprotection After Lipopolysaccharide-Induced Sepsis-Like State in Mice, (2020).
35. F.K. Mediesse, T. Boudjeko, A. Hasitha, M. Gangadhar, W.F. Mbacham, P. Yogeeswari, BMC Complementary and Alternative Medicine, (n.d.).
36. V.W. Yong, R. Moumdjian, F.P. Yong, T.C.G. Ruijs, M.S. Freedman, N. Cashman, J.P. Antel, yInterferon promotes proliferation of adult human astrocytes in vitro and reactive gliosis in the adult mouse brain in vivo, 1991.
37. A. Haque, A. Das, L.M. Hajiaghamohseni, A. Younger, N.L. Banik, S.K. Ray, Induction of apoptosis and immune response by all-trans retinoic acid plus interferon-gamma in human malignant glioblastoma T98G and U87MG cells, Cancer Immunology, Immunotherapy, 56 (2007) 615–625.
38. Ş. Çoğan, Sıçan Kemik İliğinden Ve Yağ Dokusundan Elde Edilen Mezenkimal Kök Hücrelerin Pcl Nanofibröz Yüzeyler Üzerinde Tutunma Ve Çoğalma Özelliklerinin İncelenmesi, Ege Üniversitesi Fen Bilimleri Enstitüsü , n.d.
39. Q. Yu, Y. Chen, C.-B. Xu, A convenient method for quantifying collagen fibers in atherosclerotic lesions by ImageJ software Original Article A convenient method for quantifying collagen fibers in atherosclerotic lesions by ImageJ software, 2017.
40. F. Bonnier, M.E. Keating, T.P. Wróbel, K. Majzner, M. Baranska, A. Garcia-Munoz, A. Blanco, H.J. Byrne, Cell viability assessment using the Alamar blue assay: A comparison of 2D and 3D cell culture models, Toxicology in Vitro, 29 (2015) 124–131.
41. S. Karmakar, N.L. Banik, S.K. Ray, Curcumin suppressed anti-apoptotic signals and activated cysteine proteases for apoptosis in human malignant glioblastoma U87MG cells, Neurochem Res, 32 (2007) 2103–2113.
42. H. Chen, J. Qin, Y. Hu, molecules Efficient Degradation of High-Molecular-Weight Hyaluronic Acid by a Combination of Ultrasound, Hydrogen Peroxide, and Copper Ion, (2019).
43. T. Riaz, R. Zeeshan, F. Zarif, K. Ilyas, N. Muhammad, S.Z. Safi, A. Rahim, S.A.A. Rizvi, I.U. Rehman, FTIR analysis of natural and synthetic collagen, Appl Spectrosc Rev, 53 (2018) 703–746.

44. S. Unal, S. Arslan, B. Karademir Yilmaz, F. Nuzhet Oktar, D. Ficai, A. Ficai, O. Gunduz, materials Polycaprolactone/ Gelatin/Hyaluronic Acid Electrospun Scaffolds to Mimic Glioblastoma Extracellular Matrix, Materials, 13 (2020).
45. J.W.M. Heemskerk, M.J.E. Kuijpers, L. Galgano, G.F. Guidetti, M. Torti, I. Canobbio, The Controversial Role of LPS in Platelet Activation In Vitro, (2022).
46. A. Haque, A. Das, L.M. Hajiaghamohseni, A. Younger, N.L. Banik, S.K. Ray, Induction of apoptosis and immune response by all-trans retinoic acid plus interferon-gamma in human malignant glioblastoma T98G and U87MG cells, Cancer Immunology, Immunotherapy, 56 (2007) 615–625.
47. M. Rahmati, C.P. Pennisi, A. Mobasheri, M. Mozafari, Bioengineered scaffolds for stem cell applications in tissue engineering and regenerative medicine, Adv Exp Med Biol, 1107 (2018) 73–89.
48. W. Shi, X. Zhang, L. Bian, Y. Dai, Z. Wang, Y. Zhou, S. Yu, Z. Zhang, P. Zhao, H. Tang, Q. Wang, X. Lu, Alendronate crosslinked chitosan/polycaprolactone scaffold for bone defects repairing, Int J Biol Macromol, 204 (2022) 441–456.
49. C.E. Campiglio, N.C. Negrini, S. Farè, L. Draghi, Cross-Linking Strategies for Electrospun Gelatin Scaffolds, Materials, 12 (2019).
50. G. Jensen, J.L. Holloway, S.E. Stabenfeldt, Hyaluronic Acid Biomaterials for Central Nervous System Regenerative Medicine, Cells, 9 (2020).
51. C.M. Lin, J.W. Lin, Y.C. Chen, H.H. Shen, L. Wei, Y.S. Yeh, Y.H. Chiang, R. Shih, P.L. Chiu, K.S. Hung, L.Y. Yang, W.T. Chiu, Hyaluronic acid inhibits the glial scar formation after brain damage with tissue loss in rats, Surg Neurol, 72 (2009).
52. A.C. Jimenez-Vergara, R. Van Drunen, T. Cagle, D.J. Munoz-Pinto, Modeling the effects of hyaluronic acid degradation on the regulation of human astrocyte phenotype using multicomponent interpenetrating polymer networks (mIPNs), (2020).